EUROPEAN FUSION DEVELOPMENT AGREEMENT

EFDA–JET–PR(04)34

D. Testa, M. Bigi, E.R. Solano and JET EFDA Contributors

Current Losses Induced by Edge Localised Modes in JET Tokamak Plasmas

Current Losses Induced by Edge Localised Modes in JET Tokamak Plasmas

D. Testa[1], M. Bigi[2], E.R. Solano[3] and JET EFDA Contributors*

[1] CRPP, Association EURATOM – Confédération Suisse, EPFL, Lausanne, Switzerland
[2]EURATOM/UKAEA Fusion Association, Culham Science Centre, Abingdon, OX14 3DB, UK
[3]Association EURATOM/CIEMAT, Madrid, Spain
** See annex of J. Pamela et al, "Overview of Recent JET Results and Future Perspectives", Fusion Energy 2002 (Proc.19 th IAEA Fusion Energy Conference, Lyon (2002)).*

Preprint of Paper to be submitted for publication in
Plasma Physics and Controlled Fusion

ABSTRACT.
We have investigated the effect of Edge Localised Modes (ELMs) on the total plasma current in JET tokamak plasmas using the earth leakage detection circuit connected to the in-vessel saddle coils. These measurements, and the geometry of the saddle coil circuit, indicate that, in typical H mode plasmas, up to ~300A (corresponding to a maximum of ~150A per MA of plasma current) can be deposited at each ELM in regions rather far away (~50cm) from the strike point position and divertor target plates. These current losses decrease with increasing ELM frequency (f_{ELM}), being practically below or around the detection limit for f_{ELM}>60Hz, and show some saturation for increasing diamagnetic energy losses for "slow" Type-I ELMs at f_{ELM}<10Hz. The measurements reported here are consistent with the ELM phenomenon being associated to a peeling of the edge magnetic flux surfaces.

INTRODUCTION
Edge Localised Modes (ELMs) were first observed as short bursts detected by Mirnov coils and soft-X ray diodes, associated with periodic density and temperature reduction in the outer plasma zones of H-mode plasmas [1]. Large Type-I ELMs [2] are associated with good confinementproperties, which can themselves be destroyed by the ELMs, triggering the return to the L-mode regime. The ELMs represent one of the main outstanding crucial issues for the design of ITER [3,4], as the outflux of plasma energy and particles caused by these events could prevent steady-state operation [5] and cause serious damage to the first wall [6]. Hence a lot of effort has been devoted to characterising the ELMs as function of various plasma parameters across different machines, with a particular focus on the study of their precursors [7, 8] and on the impact of the power released onto divertor target surfaces [9, 10]. Recently, there have been as well studies of current spikes in the plasma scrape-off layer associated with ELMs, measured at the divertor target plates [11], and some effort has also been spent towards controlling the ELMs via active excitation of magnetic perturbations using in-vessel coils to produce ergodisation of the divertor region [12]. In JET [12], earlier studies [14, 15] showed that Langmuir probes in the divertor target region detect current spikes at ELMs. In this work, we present data showing that current losses are detected as well far away from the divertor target area, thus expanding the information base about the off target impact of ELMs on tokamaks.

Previous JET studies [14-17] have investigated possible current losses associated with ELMs by studying the movements of the strike points. Here we consider a different approach, based on the Earth Leakage Current (ELC) detection circuit of the in-vessel saddle coils. Similar observations were reported in the autumn 1994 [18], in the early stages of saddle coil experiments on JET [19], but were considered only as a possible operational problem. At the time the data presented in this work were recorded, only the four lower saddle coils were in service in JET, labelled 1L, 3L, 5L and 7L respectively, the corresponding upper ones having been disabled in 1998. The saddle coils are large and almost completely naked metallic structures located inside (and insulated from) the vessel, facing the plasma directly without any protection on a large portion of their total surface.

The lower saddle coils are positioned below the plasma midplane, extending through 3 turns from the low to the high field side under the divertor structure, i.e. from the outer to the inner divertor leg [19]. The lower saddle coils will be disabled during the 2004-2005 JET shutdown. Figure 1(a) shows the location of the saddle coils in the poloidal cross-section of JET. Each saddle coil occupies 1/4 of the toroidal extent. The effective area of each saddle coil is $A_{EFF} = N_{TURNS}A_{SUR} \approx 75m^2$, $A_{SUR} \approx 75m^2$ being the surface area of each turn, but each saddle coil faces the plasma directly (i.e. excluding all parts covered by CFC protection tiles, under the divertor structure or in the shadow of the poloidal limiters) only through approximately 1/8 of this total area, $A_{VIEW} \approx 10m^2$. This plasma facing area is located ~50cm above the divertor target plates and the strike points for typical JET plasmas. Saddle coils at opposite toroidal locations are electrically connected and grounded in anti-series externally to the vacuum vessel. Each of the two pairs of saddle coils has a single connection to the JET earth, equipped with an ELC measurement, for a total of two independent ELCs. Figure 1(b) show a schematic toroidal cross-section of JET with a layout of the ELC detection circuit. The saddle coil earth current transducer concentrates in a magnetic circuit the magnetic flux proportional to the ELC, which is then measured in an air gap by a Hall effect device. This sensor, located on the cabling about 80m away from the saddle coils and externally to the Torus hall, detects the current flowing from the saddle coil circuit to machine earth with a 1kHz sampling rate. Each Type-I ELM is individually observed with this sampling rate but, on the contrary, blending in the ELC measurements between subsequent events sometimes occurs for very frequent Type-III ELMs. The practical detection limit of any ELC above the noise level is around ~10A, and only about 30% of the observed Type-III ELMs in JET have ELC signals above this empirical threshold.

The design of the saddle coils is such that the coils are electrically insulated from the vessel. Hence, if short circuits to machine earth were permanent and/or low impedance, any magnetic perturbation associated to a floating potential $V = A_{EFF}\,\partial B/\partial t$ would induce an ELC in the saddle coils, contrary to the existing measurements. Similarly, flow of neutral gas through the saddle coils cannot cause current flow or short circuits to machine earth. The other circumstances when an ELC is measured in the saddle coils is during disruptions and active operation, i.e., when an external power supply feeds the saddle coils. Hence the measurement of an ELC in the saddle coils during passive operation must be attributed to plasma shorting the coils to vessel and winding its way back through machine earth. Thus we conclude that the ELC measured in the saddle coils synchronously with ELMs is associated with a net current flowing from the plasma itself to vessel potential, most likely coming from a region at the plasma edge due to the saddle coil geometry and their position. The total current measured on a pair of saddle coils is the net signed sum of the current detected on each one of the two saddle coils, and it is indeed possible to measure the partial contribution of each coil of one pair to the total ELC. Each saddle coil is equipped with a differential current Rogowski coil, located on the cabling 80m upstream of the coil, outside the Torus hall. The differential current Rogowski coil measures the difference between the current flowing in the two coil's feeds (see Fig.1(b)), one feed being connected to the inner divertor leg and the other feed to the outer divertor

leg, i.e., the high or low field side, respectively, depending on the circuit arrangement. It should be noted that this sign convention is absolute, i.e., it is not related to the direction of the plasma current in JET (neither local current density nor total volume-integrated value). Hence the sign of the measured ELC on one individual saddle coil indicates where most of the current was detected at the ELM (low/high field side, outer/inner divertor leg, respectively). However, due to the saddle coil geometry, it is not possible to determine if the current measured in the ELC circuit was originally flowing in the toroidal, poloidal or radial direction. In our experimental conditions, the positive conductor is always disconnected from the power supplies with no current path available. Hence, any current measured by the differential current Rogowski can only be flowing through the negative conductor, connected to the machine earth. This provides a way to discriminate the contribution of each coil to the total earth current measured for the pair, according to Kirchoff's current law as applied to the nodes labelled "1" and "2"in Fig.1(b). We should point out that the ELC measurements and the differential current measurements do indeed add up according to Kirchoff's current law. We believe that this agreement between measurements taken from different transducers, of different nature and at different locations external to the tokamak hall, obviously with no possibility of any direct magnetic coupling to the plasma, provides an extremely convincing argument that these measurements do arise from the actual flow of electrical current in the saddle coil earth circuit.

Figure 1(b) further elucidates one of the main features of the results reported here: the sign of the measured ELC can be opposite for the two pairs of saddle coils and can change sign during the same discharge for one pair of saddle coils depending on where most of the current is detected (i.e., low or high field side, outer or inner wall, respectively). As an illustration of this feature, Fig.2 shows an example of the ELC measurement for Pulse No: 60532, an H-mode discharge with low-frequency Type I ELMs, $f_{ELM} \sim 6$Hz. The insert zooms around the ELM event at t = 10.6sec, showing the ELC measurements for each individual saddle coil. The earth leakage current is initially detected on the high field side (ELC1<0 and ELC3<0, ELC5>0 and ELC7>0, respectively), then on the low field side (ELC1>0 and ELC3>0, ELC5<0 and ELC7<0, respectively). This provides in principle an indication of the in/out asymmetry (toroidal, poloidal) in the distribution of the current measured by the saddle coil ELC detection circuit during certain, but not all, ELMs. For example, the current loss is symmetric and does not switch polarity for the ELM occurring at t=10.4sec in Pulse No: 60532. For Type-I ELMs the position where the current is initially lost is approximately equally split between the inner and outer wall; then in about half of the cases considered here, mostly corresponding to low-frequency ELMs with f_{ELM}<10Hz, we have observed this position to flip side at the next time point in the ELC measurements, occurring 1ms later. Thus, possibly owing to the somewhat poor time resolution of the ELC measurements (1kHz), we conclude that there is no preferential position (inner/outer wall) for where the current lost is deposited on material surfaces. Note also that this sampling time is also much longer than the time that would take lost electrons or ions to reach the saddle coils, estimated to be ~1ms for the electrons and ~40μs for the ions: hence the measured ELC is to be intended as a partial loss of plasma current in the broader sense of the

signed current carried by moving charged particles that are ejected from the plasma at the occurrence of an ELM.

Figures 3(a) and 3(b) show the main plasma parameters and the measured ELC and diamagnetic energy W_{DIA} associa ted to more frequent (f_{ELM} ~ 20Hz) Type-I ELMs for Pulse No: 62490, an H-mode plasmas with Neutral Beam Heating (NBI) in the hybrid tokamak scenario [20], with a monotonic q-profile and q_0>1. For Type-I ELMs, up to ~300A can be lost at each ELM over the plasma viewing area of the saddle coils. Similar measurements for discharges with Type-II and Type-III ELMs indicate that the ELC does not usually exceed ~25A, if any at all. For fast (f_{ELM} > 60Hz) Type-II and Type-III ELMs, the current loss is too small to be associated to any significant (i.e., directly measurable outside the error bar) change in the internal inductance l_i. For slow and bigger Type-I ELMs such as those in Pulse No: 60532, we do, on the other end, indeed observe some minor changes in l_i, typically $\Delta l_i \approx 0.05$ per 100A of ELC. The loop voltage data is not available on a fast enough time scale (the measuring loop is outside the vessel) and the plasma current is not directly measured in JET, thus no firm conclusions on possible changes in these quantities due to the ELMs can be drawn.

As a possible explanation for the measurements reported here, we start by considering the usual model of transport associated with ELMs, which is described, for instance, in Refs.[21]. The ELM produces a substantial increase of the radial transport of particles and energy across the separatrix onto the open field lines of the scrape-off layer, while the magnetic topology is assumed to be unchanged over the fast ELM time-scale. Particles and energy then flow along the open field lines towards the target plates. Such a model might explain the observed target plate currents [11, 14]. On the other hand, it would be rather difficult to imagine that flow along well-behaved field lines in the plasma scrape-off layer would take edge plasma current to a remote location from the separatrix, as presented here. An alternative model of the ELM, as illustrated in Refs.[16, 17], could be consistent with our observations. An ELM can be modelled as a peeling of closed flux surfaces, due to a fast growing instability in a fragile equilibrium [22]: the pre-ELM separatrix breaks, some edge current is lost and a new separatrix forms, enclosing a smaller plasma volume. The process could indeed be symmetric, in the form of a peeling of a whole layer of plasma. However, it is conjectured here that it is more likely for such peeling to occur in ribbons or flux tubes, which peel-off from the plasma edge and undergo an erratic motion, obeying local dynamic equations until a conducting surface is encountered and the current is discharged, as for instance experimentally observed in ASDEX-U [23] and MAST [24]. This is consistent with the observation, reported here, of plasma current being lost further away from the separatrix and the strike point regions. Some evidence of filaments expelled from the plasma towards the vessel wall during ELMs is also indeed available in JET via visible imaging [25], but unfortunately the camera views the top of vessel, i.e., far away from the position of the saddle coils.

Table 1 provides an overview of the main plasma data for four typical examples of ELM behaviour: the corresponding ELC and W_{DIA} data are plotted in Fig.4. The (toroidal, poloidal) asymmetry in the

current loss distribution is particularly clear for the discharges with Type-I ELMs. For the selected time-slice for Pulse No: 63278, a pulse with high-frequency (f_{ELM}~150Hz) Type-III ELMs, we also notice an almost exact cancellation of the currrent lost on the inner/outer wqall for the saddle coil pair 3-7. Many well-established theory-based models and empirical scaling laws already exist for the relation between the diamagnetic energy losses and the ELM frequency and other plasma parameters, such as the edge collisionality and safety factor, and the pedestal density, temperature and pressure (see as example Refs.[26-29]). Thus, a detailed theoretical or numerical modelling of the experimental results presented here is beyond the scope of this work. In order to stimulate such activities, the database summarising our measurements is presented in Table 2 and fig.5, which shows the scaling of the ELC measurements as function of the diamagnetic energy losses and ELM frequency. The complete database contains 828 points, and is rather sparse, with a large variation in the edge safety factor, $2.7 < q_{95} < 7.9$, the edge triangularity, $0.25 < \delta_{95} < 0.45$, and the edge density and temperature, $1.1 < n_e^{95}(10^{19}\ m^{-3}) < 9.8$ and $0.2 < T_{e95}(keV) < 1.6$, respectively. Here the subscript "95" indicate that the data is taken at the radial position $\sqrt{\psi_N} = 0.95$, where ψ_N is the normalised poloidal flux.

The various background plasma data presented in Table 2 demonstrate that ELC associated with ELMs, such as they are, is measured in a large variety of situations. To avoid possible blending in the ELC measurements, only well-resolved Type-III ELMs, i.e. those with fELM<400Hz, have been included in this database. For clarity in the presentation of the data reported here, we have restricted the selection* presented in Table 2 and fig.5 to points with edge triangularity $0.34 < \delta_{95} < 0.43$, which was achieved for an edge elongation $1.68 < \kappa_{95} < 1.77$, and averaged the various data points associated to each resulting value of ΔW_{DIA} and f_{ELM}. This process helps us in avoiding unnecessary cluttering in fig.5, since many very similar (i.e. within 10% scatter) ELC, ΔW_{DIA} and f_{ELM} points are obtained for very different values (i.e., with more than 35% scatter) of the edge density and temperature. Our selection criteria is thus based on δ_{95} for two reasons: (a) there is clear operational evidence in JET [24-26] that the ELM behaviour is affected by δ_{95}, and (b) this selection allows us to retain the database marginals (i.e., the global probability function in the reduced database for the measured ELC to be in a certain range of ΔW_{DIA} and f_{ELM} once the other background plasma parameters are given does not change by more than half its standard deviation in the original database).

Since we have considered here a f_{ELM} defined as the number of ELMs per second over the steady-state time window of interest, we have taken this datum to be free from statistical errors. The relative error on ΔW_{DIA} ($\sigma_{\Delta W}$) and ELC (σ_{ELC}) are thus determined by the uncertainties in the raw measurements, ~10% on W_{DIA} and ~30% on ELC, to which we have then added the scatter in the "original" data. Note that this scatter was implicitly smoothed out through the averaging process over ΔW_{DIA} and f_{ELM}. This approach reduces the complete 828-points database to 28 and 25 individual ΔW_{DIA} and f_{ELM} data points, respectively, covering the range $0 < \Delta W_{DIA}(MJ) < 0.9$ and $7 < f_{ELM}(Hz) < 400$, still with some scatter in the edge safety factor, $3.1 < q_{95} < 6.4$, density and temperature, $1.8 < n_{e95}\ (10^{19}\ m^{-3}) < 7.3$ and $0.25 < T_{e95}(keV) < 1.5$, respectively. Alternative or additional methods to

consolidate the 828-points database have been rejected since they reduce unnecessarily the statistics on the ELC data. For clarity in Fig.5, we did not plot the ELC data for $f_{ELM} > 60$Hz since in these regimes the measured ELC is approaching its detection limit, ELC~10A. For low frequency, hence mostly Type-I, ELMs the current losses decrease with increasing ELM frequency, with an ELC $\propto 1/f_{ELM}$ trend. The value $\Delta W_{DIA} \sim 0.2$MJ indicates a boundary between Type-III and Type-I ELMs: the ELC increases almost linearly with ΔW_{DIA} up to ΔW_{DIA}~0.5MJ, and possibly shows a saturation above ΔW_{DIA}~0.6MJ, where the ELC is practically constant for ΔW_{DIA} increasing up to ΔW_{DIA}~0.9MJ. We have however very few points in total (31 out of 828) in our database with ΔW_{DIA}>0.5MJ and ELC > 200A. Hence this result, which may indicate different and additional dependencies on other plasma parameters, such the edge temperature, density and q_{95} (which were very clearly not matched between different discharges in our database), as function of the ELM size, is of a rather more tentative nature.

In summary, we have provided experimental evidence indicating that, in typical H-mode JET plasmas, up to ~300A (corresponding to up to a maximum of ~150A per MA of plasma current) can be lost at each Type-I ELM crash and deposited in regions rather far away from the strike point and divertor target plates position. These losses occur over the plasma viewing area of the saddle coils, which views approximately 1/8 of the total edge plasma surface. The current losses distribution shows some indication of toroidal and poloidal asymmetry for certain, but not all, low-frequency Type-I ELMs, suggesting topological differences between otherwise apparently very similar events. The presence of current losses caused by the ELMs rather away from the divertor region provide additional evidence that the ELM phenomenon is associated to a new equilibrium being established at the plasma edge, and suggests that the ELMs are linked to a peeling of the edge flux-surfaces.

ACKNOWLEDGEMENTS

The authors would like to acknowledge the contribution of the whole JET experimental team, and in particular S.Arshad, A.Cenedese, J.Conboy, G.Saibene and R.Sartori. Our special thanks go to Dr.Emilia Solano and Dr.Phil Edmonds for their advice and comments on this work, to Dr.Eric Gauthier for his advice on visible imaging of ELMs on JET and to the Referees for their help in clarifying various points in the initial presentation of our results. This work has been conducted under the European Fusion Development Agreement. D.Testa was partly supported by the Fond National Suisse pour la Recherche Scientifique, Grant 620-062924.

REFERENCES.

[1]. F.Wagner et al., Phys. Rev. Lett. **49** (1982), 1408.

[2]. H.Zohm, Plasma Phys. Controlled Fusion **38** (1996), 105.

[3]. R.Aymar et al., Plasma Phys. Controlled Fusion **44** (2002), 519.

[4]. ITER Physics Basis Editors, Nucl. Fusion **39** (1999), 2137; 2004 issue, in preparation.

[5]. A.Loarte et al., Extrapolating type-I ELMs physics to ITER, to appear in the Proceedings of

the 11th European Fusion Physics Workshop, Heraklion, Crete, 8-10 December 2003.
[6]. G.Federici, ITER JWS Group, Plasma-wall interaction in ITER, to appear in the Proceedings of the 11th European Fusion Physics Workshop, Heraklion, Crete, 8-10 December 2003.
[7]. C.Perez et al., Type-I ELM precursor modes in JET, Nucl. Fusion **44** (2004), 609.
[8]. J.Lonnroth et al., Plasma Physics and Controlled Fusion **46** (2004), 767.
[9]. A.Loarte et al., Plasma Phys. Control. Fusion **44** (2002), 1815.
[10]. G.Federici et al., Plasma Phys. Control. Fusion **44** (2002), 1523.
[11]. H.Takahashi, Observation of current in SOL plasma and possible roles played by associated error field in AT discharges in DIII-D tokamak, Proceedings 30th EPS Conference on Controlled Fusion and Plasma Physics, St.Petersburg, 7-11 July 2003 (ECA Vol. 27A, P-3.178).
[12]. T.Evans et al., Phys. Rev. Lett. 92 (2004), 235003.
[13]. J.Wesson, Tokamaks, 3rd edition, (Oxford Science Publication, Oxford, 2003), p.617.
[14]. J.Lingertat et al., Studies of giant ELM interaction with the divertor target in JET, Proceedings 22nd EPS Conference on Controlled Fusion and Plasma Physics, Bournemouth, 3-7 July 1995.
[15]. S.Arshad et al., Plasma movements at ELMs in JET, internal JET Report, 1995 (available upon request to duccio.testa@epfl.ch).
[16]. E.R.Solano et al., Current loss and strike point movement during ELMs in JET, Proceedings 30th EPS Conference on Controlled Fusion and Plasma Physics, St.Petersburg, 7-11 July 2003 (ECA Vol. 27A, P-1.106).
[17]. E.R.Solano et al., ELMs and strike point jumps, to appear in the Proceedings 16 th Conference on Plasma Surface Interaction, Portland, USA, 24-28 May 2004.
[18]. M.De Benedetti, internal JET memorandum, JET Joint Undertaking, 1994 (available upon request to duccio.testa@epfl.ch).
[19]. A. Santagiustina et al., Operational experience with the JET saddle coil system, Proceedings of the 19th Symposium on Fusion Technology, Lisbon, 16-20 September 1996, Vol.1 p.989.
[20]. C.Gormezano et al., "Hybrid advanced scenarios: perspectives for ITER and new experiments with dominant ICRF heating", 31st EPS Conference on Controlled Fusion and Plasma Physics, London, 28 June to 02 July 2004; to appear in Plasma Physics and Controlled Fusion, 2004.
[21]. J.Connor, Plasma Phys. Control. Fusion 40 (1998), 531; M.Fenstermacher et al., Plasma Phys. Control. Fusion 45 (2003), 1597; M.Becoulet et al., Plasma Phys Control. Fusion 45 (2003), A93.
[22]. E.R.Solano, Plasma Phys. Control. Fusion **46** (2004), L7.
[23]. T.Eich et al., Phys.Rev. Lett. **91** (2003), 195003.
[24]. A.Kirk et al., Phys. Rev. Lett. **92** (2004), 245002.
[25]. Eric Gauthier, private communication, JET Facilities, December 2004.
[26]. L.Horton et al., Nuclear Fusion **39** (1999), 1.
[27]. R.Mohanti et al., Statistical analysis of Type-I ELMs at JET, Proceedings 24th EPS Conference on Controlled Fusion and Plasma Physics, Berchtesgaden, 7-11 July 1997.
[28]. R.Sartori et al., Plasma Phys. Control. Fusion **46** (2004), 723.
[29]. A.Loarte et al., Physics of Plasmas **11** (2004), 2668.

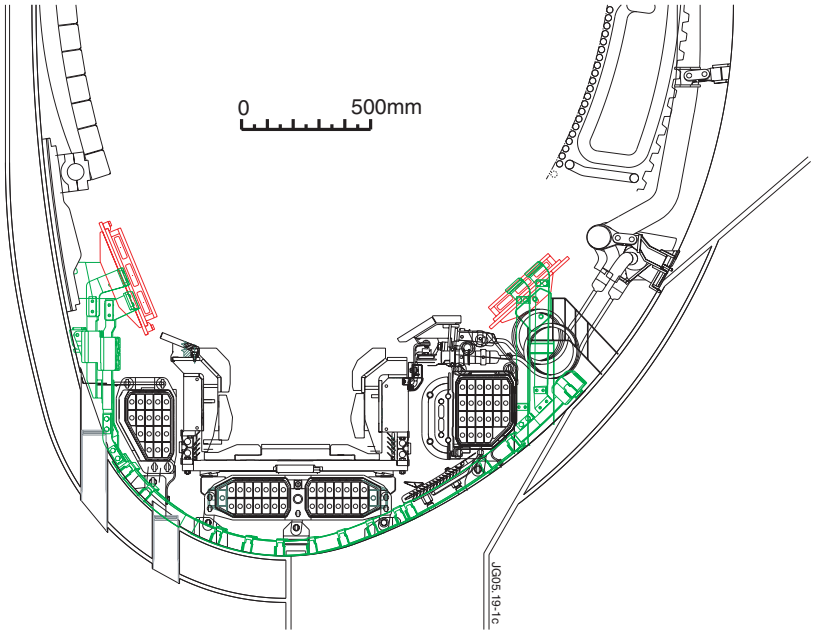

Figure 1(a): Poloidal cross-section of the JET tokamak, showing the geometrical assembly of one the lower saddle coils, extending from the low to the high field side below the divertor structure. The parts of the saddle coils which are (not) directly exposed to the plasmas are colour-coded in green (not exposed) and red (exposed), respectively.

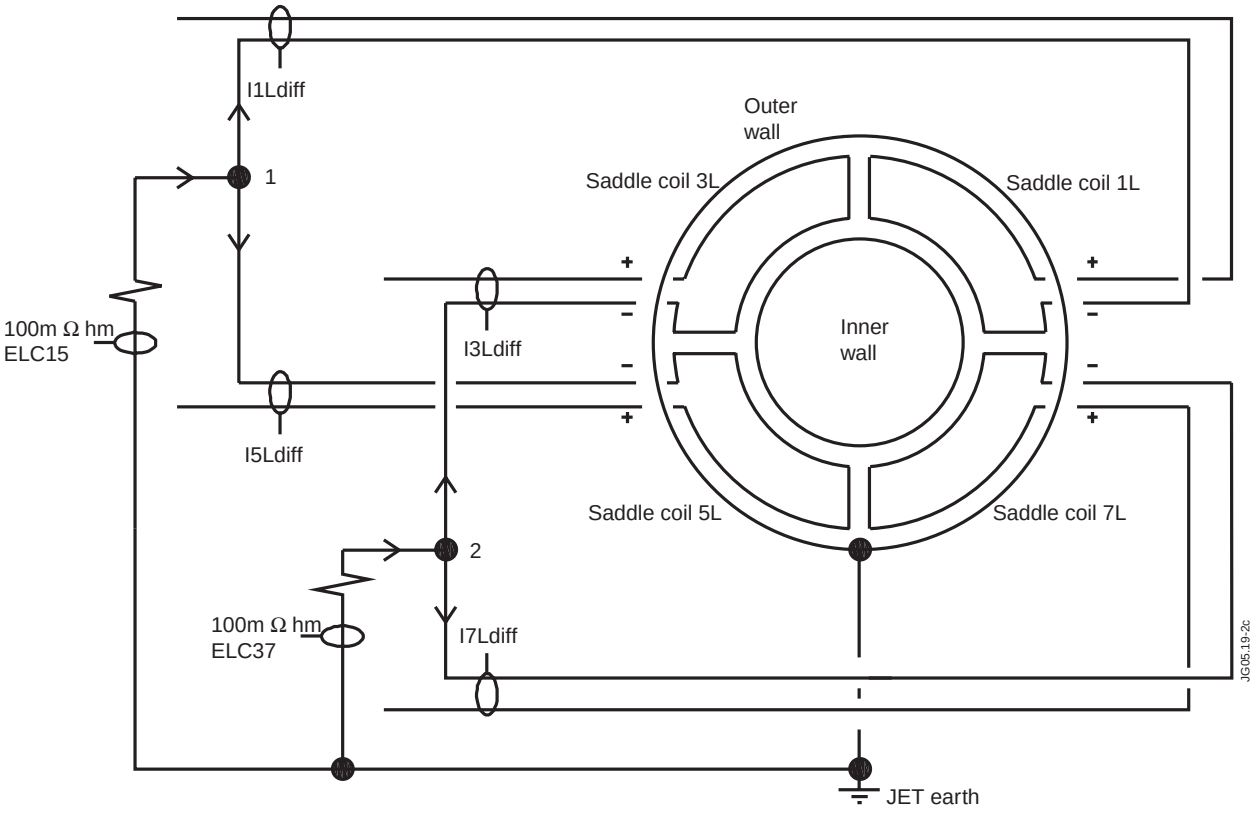

Figure 1(b): Schematic toroidal cross-section of JET, showing the layout of the earth leakage current detection circuit for the two pairs of saddle coils. The lost current in the saddle coils is measured through a Hall effect device.

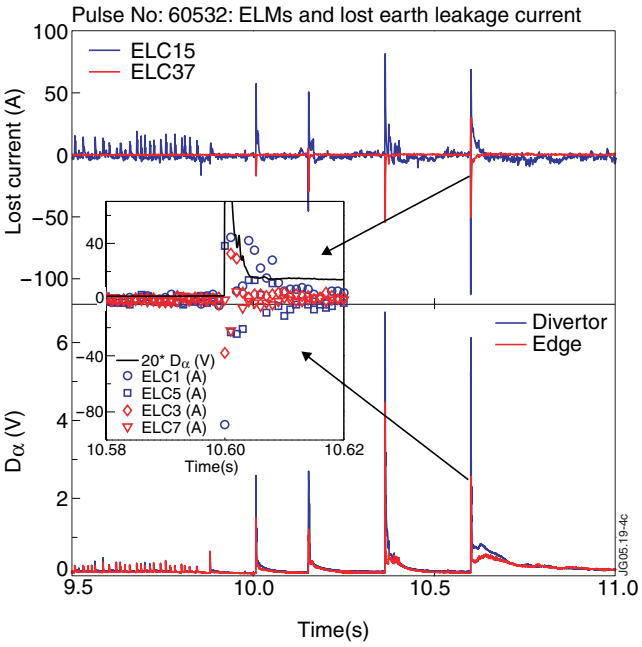

Figure 2: Synchronisation between ELMs and earth leakage current in the saddle coil circuit for low-frequency Type-I ELMs. Here ELCmn indicates the ELC measurement for the saddle coil pair mn. ELCm indicates the ELC of the individual m saddle coil as measured by the differential current Rogowski coil. Note the different and time-varying sign of the ELC measurements, which indicates poloidal and toroidal asymmetry in the current loss distribution. The insert zooms around the ELM at t = 10.6sec to show the detailed time-evolution of the ELC and D_α signals.

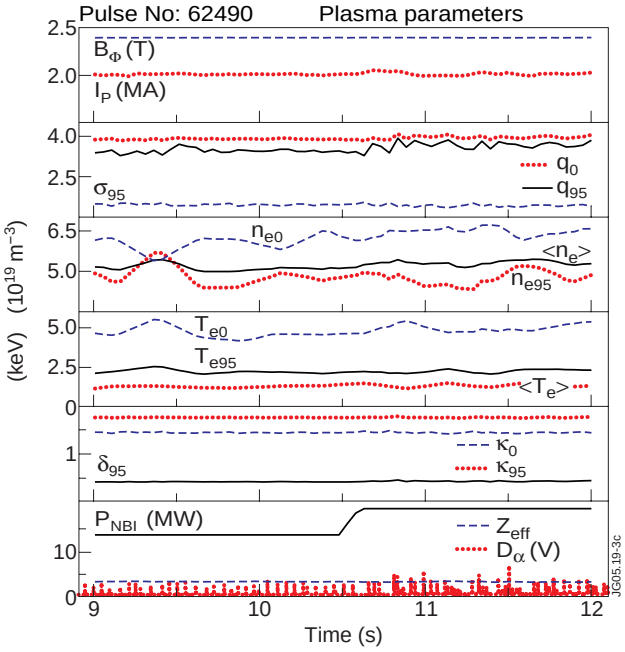

Figure 3(a): Main plasma parameters for Pulse No: 62490, a JET H-mode plasmas with NBI heating and Type-I ELMs, with a monotonic q-profile and $q_0>1$. Here q_{95} and σ_{95} are the safety factor and its shear, $\sigma = (r/q)(dq/dr)$, at the plasma edge, $\sqrt{\psi_N} = 0.95$; ψ_{95} and δ_{95} are the edge elongation and average triangularity (lower/upper midplane); n_{e0}/T_{e0}, n_{e95}/T_{e95} and $<n_e>/<T_e>$ are the central, edge and volume-averaged electron density and temperature; Z_{EFF} is the effective plasma charge and $B\phi$ and I_p are the on-axis magnetic field and plasma current.

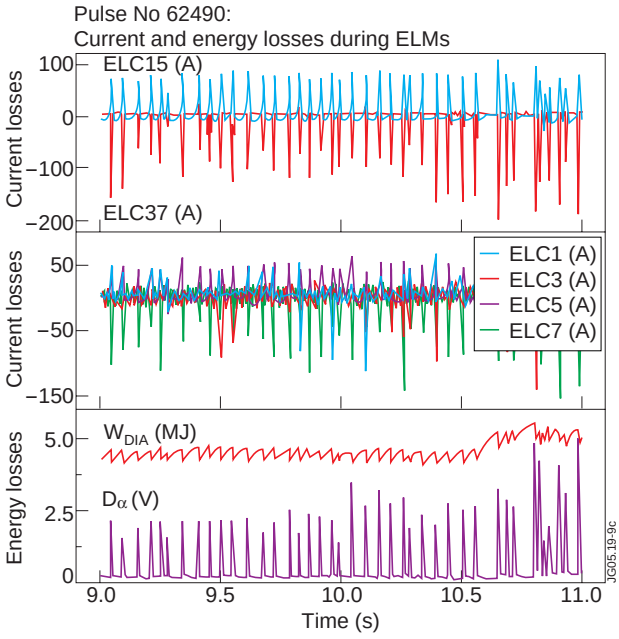

Figure 3(b): Measurement of the current and diamagnetic energy losses for Pulse No: 62490. Up to ~300A can be lost at each Type-I ELM crash over the plasma viewing area of the saddle coils, located approximately 50cm above the strike point position.

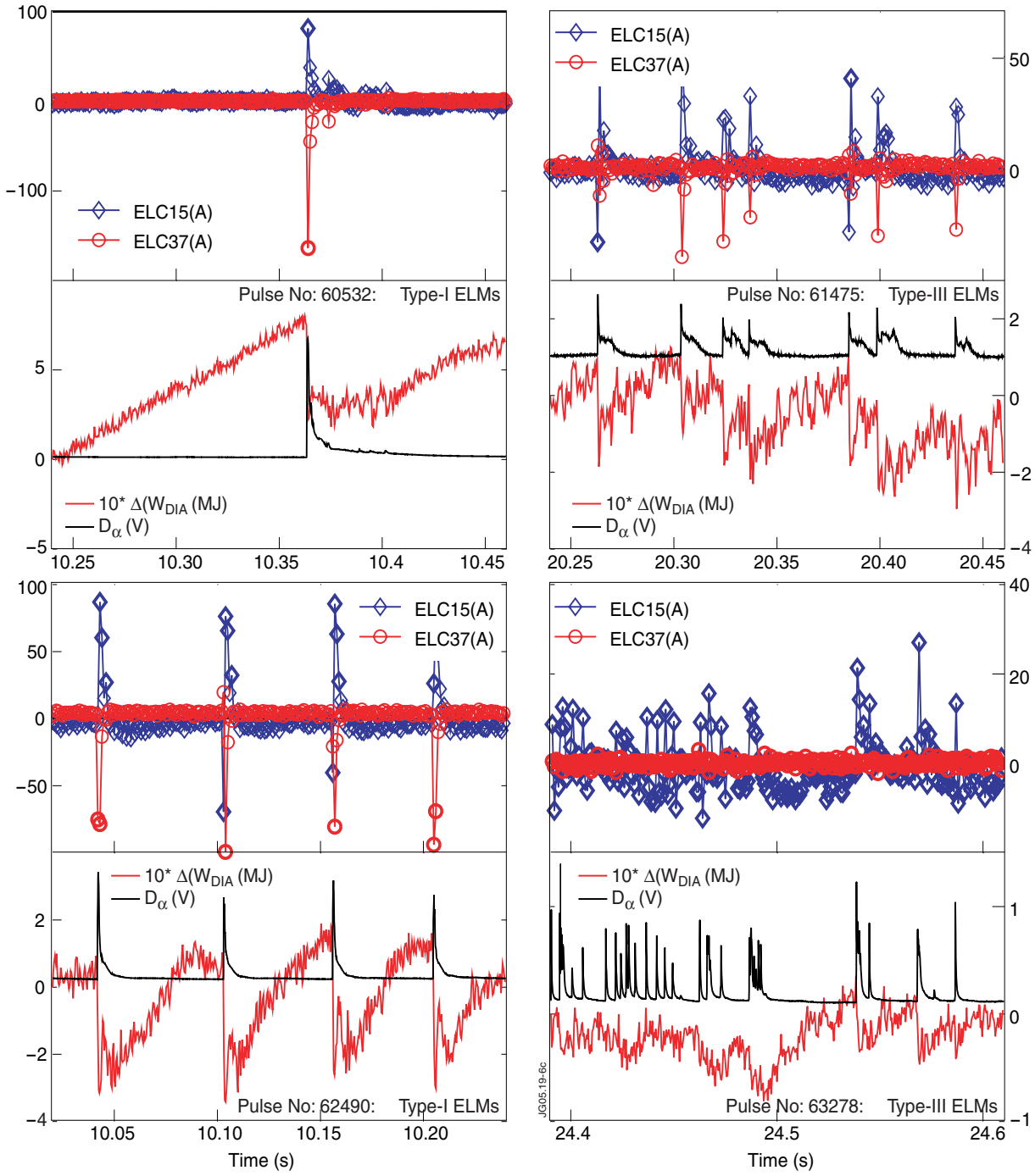

Figure 4: Overview of the ELC measurements for the four typical examples of ELM behaviour, as considered in Table 1. Note that some blending in the ELC measurements occurs for very fast Type-II and Type-III ELMs, typically with f_{ELM}>400Hz.

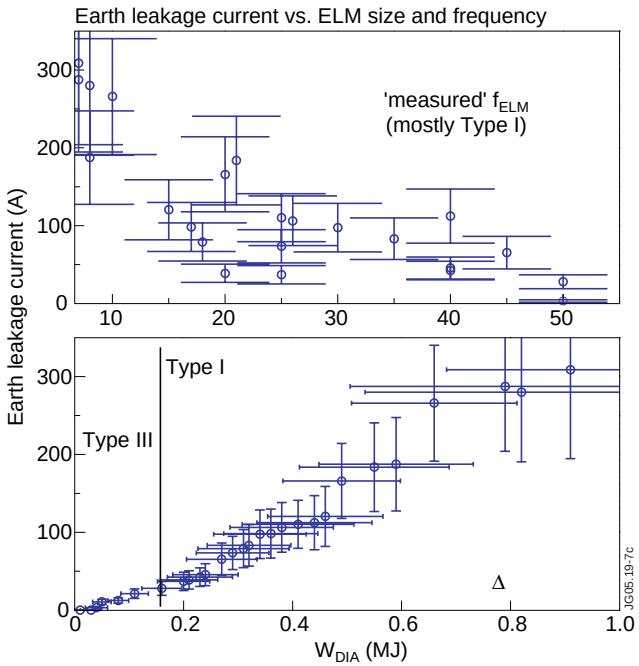

Figure 5: Scaling of the earth leakage current measurements as function of the diamagnetic energy losses and measured ELM frequency for the database considered in this work, with edge safety factor $3.1_{95} < q_{95} < 6.4$, triangularity $0.34 < \partial_{95} < 0.43$ and elongation $1.68_{95} < \kappa_{95} < 1.77$.

Pulse No:	Time	Type	f_{ELM}	ELC	ΔW_{DIA}	P_{NBI}	I_P	B_ϕ	n_{e95}
	(sec)		(Hz)	(A)	(kJ)	(MW)	(MA)	(T)	(10^{19} m^{-3})
62490	10.16	I–fast	20	175	360	13.5	2.0	2.4	4.9
60532	10.36	I–slow	6	210	550	15.5	3.4	2.7	4.7
61475	20.30	II	40	70	120	13.6	2.5	2.7	8.1
63278	24.54	III	150	20	90	4.9	0.9	1.2	1.9

JG05.19-10c

Table 1: Overview of the main plasma data for four typical examples of ELM behaviour

ΔW_{DIA}	ELC	I_p	P_{NBI}	δ_{95}	q_{95}	f_{ELM}	B_ϕ	κ_{95}	n_{e95}	T_{e95}	W_{DIA}	$\sigma_{\Delta W}$	σ_{ELC}
(MJ)	(A)	(MA)	(MW)			(Hz)	(T)		($10^{19}m^{-3}$)	(keV)	(MJ)	(rel)	(rel)
0.01	0.0	0.68	1.99	0.39	4.18	400	0.94	1.68	1.72	0.25	0.29	1.00	1.00
0.03	0.0	0.83	3.89	0.39	3.74	400	1.00	1.73	2.00	0.37	0.62	0.65	0.70
0.04	3.2	0.92	4.15	0.35	3.56	50	1.06	1.72	2.14	0.39	0.73	0.51	0.50
0.05	10.6	0.83	3.85	0.38	3.74	250	1.00	1.73	2.01	0.37	0.62	0.34	0.31
0.08	12.5	1.19	4.93	0.26	3.12	120	1.24	1.71	2.62	0.51	1.06	0.24	0.27
0.11	21.2	1.52	7.60	0.37	3.56	170	1.69	1.75	4.26	0.62	2.50	0.23	0.29
0.16	28.0	1.85	11.88	0.41	5.31	50	2.68	1.70	5.37	1.10	3.89	0.23	0.32
0.20	37.0	2.25	12.34	0.39	3.58	25	2.43	1.73	6.02	1.07	4.75	0.24	0.32
0.21	38.9	2.17	11.98	0.41	4.23	20	2.53	1.72	6.71	1.11	4.57	0.25	0.30
0.23	42.4	2.00	12.36	0.41	4.89	40	2.68	1.71	5.64	1.01	4.36	0.26	0.28
0.24	45.6	2.44	12.45	0.41	3.40	40	2.44	1.74	7.35	1.06	5.06	0.25	0.31
0.27	65.3	2.36	14.04	0.41	3.69	45	2.60	1.74	6.80	1.15	5.36	0.24	0.32
0.29	73.5	2.30	12.70	0.41	3.43	25	2.28	1.76	6.23	1.05	4.72	0.23	0.29
0.31	79.1	2.00	16.46	0.42	3.93	18	2.39	1.77	4.70	1.34	4.75	0.27	0.31
0.32	83.3	1.66	14.87	0.42	5.45	35	2.56	1.72	3.60	1.17	3.77	0.24	0.32
0.34	97.5	2.08	15.95	0.42	3.87	30	2.43	1.76	5.29	1.24	4.86	0.25	0.32
0.36	98.3	2.33	14.18	0.40	4.01	17	2.61	1.74	6.37	1.19	5.20	0.24	0.32
0.38	106.3	2.32	14.64	0.42	3.74	26	2.57	1.75	6.86	1.14	5.41	0.25	0.30
0.41	110.2	2.11	16.96	0.42	4.09	25	2.51	1.75	5.43	1.19	5.06	0.25	0.28
0.44	112.3	1.60	15.99	0.43	5.52	40	2.53	1.73	3.44	1.30	3.75	0.24	0.31
0.46	120.4	1.53	15.33	0.43	5.81	15	2.56	1.72	3.24	1.41	3.53	0.23	0.32
0.49	166.0	1.71	16.03	0.43	5.21	20	2.53	1.73	3.96	1.38	4.03	0.22	0.29
0.55	183.7	1.95	13.22	0.41	4.19	21	2.39	1.76	4.74	1.26	4.16	0.25	0.31
0.59	187.4	1.40	11.78	0.43	6.44	8	2.57	1.69	3.05	1.49	2.73	0.24	0.32
0.66	265.8	2.37	8.68	0.41	3.24	10	2.07	1.76	6.32	0.94	4.09	0.23	0.28
0.79	287.4	2.21	2.75	0.36	3.49	7	2.07	1.73	5.50	1.05	3.70	0.36	0.29
0.82	280.0	2.14	1.32	0.34	3.61	8	2.07	1.72	5.25	1.11	3.17	0.35	0.32
0.91	308.8	2.21	2.75	0.36	3.49	7	2.07	1.73	5.50	1.05	3.59	0.25	0.37

JG05.19-8c

Table 2: Summary database for the experimental results presented here.